

MARE BASALT GENESIS: TRACE ELEMENTS AND ISOTOPIC RATIOS; A.B. BINDER,  
Senior NRC Fellow, Johnson Space Center, TX 77058

Earlier analysis (1) of the major oxide, siderophile element (Ni and Co), and incompatible element (Ba and the REE) data for the mare basalts suggested the following model of the formation of their magmas: The primary magmas formed by olivine controlled,  $30 \pm 2\%$  partial melting of shallow ( $< 200$  km), olivine dominated, density graded source regions. The magmas rose to the crust-mantle boundary where they pooled in magma chambers. As the primary magmas cooled in the chambers, they lost 0-30% olivine or 30% olivine + 0-30% pyroxene by fractional crystallization, and gained most of their incompatible elements by the assimilation of 0-10% of UrKREEP residuals (residuals from the partial, fractional remelting of UrKREEP) from the chamber walls. This model accounts for the wide variations in the olivine and ilmenite contents of the mare materials, their varied Ba, REE, Ni, and Co distribution patterns and concentrations, and other characteristics.

As an extension and test of this model, I have expanded the modelling described in (1) to include the data for A) additional incompatible elements for which distribution coefficients are available [K, Rb, and Sr] and B) the Rb-Sr and Sm-Nd isotopic systems. I have also taken into account the effects on the trace element concentrations in the basalts by A) the incorporation of small amounts [0-10%] of trapped melt in the cumulating crystals which formed the density graded layers of the source regions and B) the remelting and simultaneous deposition of crystals from the convecting magma system [magma ocean] as the basalt source region and crust formed. The latter was achieved by the development of a new set of trace element distribution equations.

The refined calculations show that the proposed model successfully accounts for the concentrations and distribution patterns of the 12 incompatible elements studied and the Rb-Sr and Sm-Nd isotopic ratios of almost all mare basalts. Further, the model also accounts for the systematic decrease of the Ni contents of the pyroclastic glasses with increasing  $TiO_2$  content observed by Delano [see Fig. 6.24 of (2)]. The latter is an effect of the remelting of the crystals along the bottom of the convection cells as modelled by the newly developed distribution equations. The model calculations also show that the Sr and Eu content of the magmas were mainly controlled by the amounts of Sr and Eu in the source regions and therefore these two elements act as source region tracers. In contrast and as shown earlier (1), the amounts and depletion patterns of the remaining 10 incompatible elements studies are controlled by A) the amount of UrKREEP assimilated by the primary magmas and B) the degree of partial, fractional remelting the UrKREEP had undergone. These results indicate that the Rb-Sr systematics are controlled by a complex interplay of the Rb-Sr concentrations and evolution in both the source regions and in the UrKREEP residuals, while the Sm-Nd systematics are mainly controlled by the Sm-Nd concentrations and evolution in the UrKREEP residuals. Despite these complexities, the model successfully accounts for the isotopic systematics of both of these systems.

Examples of these new results are given in Figs. 1 and 2. Fig. 1 depicts the observed and model distribution patterns of the incompatible elements of 5 representative mare units. Also shown in Fig. 1 are the observed and model patterns of KREEP and the average highland anorthosite; the latter is important since any successful model of the mare basalt source region and mare basalt genesis must be able to explain the characteristics of the cogenetic highland rocks. Fig. 2 gives an example of the observed and model initial values of the

## MARE BASALT GENESIS

Binder, A.B.

$^{87}\text{Sr}/^{86}\text{Sr}$  vs  $^{143}\text{Nd}/^{144}\text{Nd}$  for 3 mare units. The success of the proposed model in accounting for the expanded set of data, especially the isotopic data, adds considerable support to the proposed model.

## REFERENCES:

- (1) Binder, A.B. (1982) Proc. Lunar Planet. Sci. Conf. 13, p. A37- A53.
- (2) Taylor, S.R. (1982) Planetary Science: A Lunar Prospective, The Lunar and Planetary Institute, p. 332.

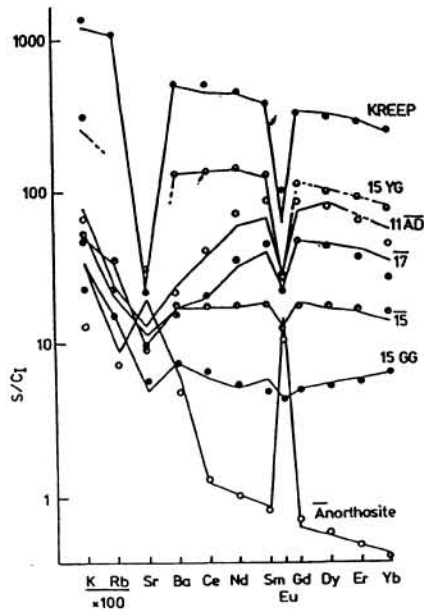


Fig. 1. Observed (continuous lines) and model (filled, partially filled, and open circles) incompatible element distribution patterns for 5 mare units, KREEP, and anorthosites.

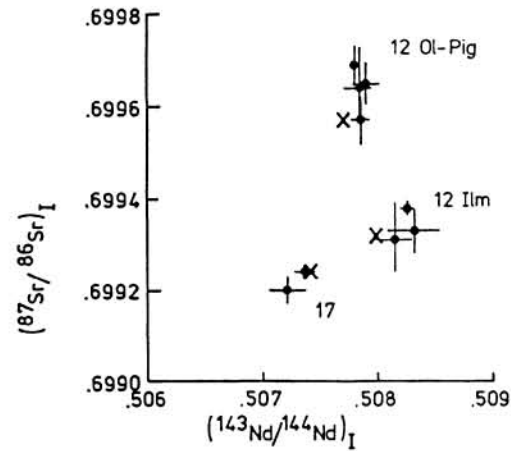


Fig. 2. Observed (filled circles with error bars) and model (X's) initial  $^{87}\text{Sr}/^{86}\text{Sr}$  vs  $^{143}\text{Nd}/^{144}\text{Nd}$  values for 3 mare units.